MBoC | ARTICLE

Divisome and elongasome organisation in the genome-reduced obligate intracellular bacterium *Orientia tsutsugamushi*

Suthida Chuenklin[a,b,†,#], Elizabeth Harris[a,#], Owen Somhorst[a,c], and Jeanne Salje[a,b,c,d,*]
[a]Cambridge Institute for Medical Research, University of Cambridge, CB2 0XY Cambridge; [b]Mahidol-Oxford Tropical Medicine Research Unit, Faculty of Tropical Medicine, Mahidol University, Bangkok, 10400 Thailand; [c]Department of Pathology, University of Cambridge, CB2 1QP Cambridge; [d]Department of Biochemistry, University of Cambridge, CB2 1GA Cambridge

ABSTRACT **Cell elongation and cytokinesis are mediated by two large multi-protein complexes in rod-shaped bacteria: the elongasome and divisome. These membrane-associated complexes ultimately recruit peptidoglycan cell wall remodeling and synthesis machineries, thus sculpting and extending growing cells or driving septation of two daughter cells. The elongasome and divisome have been well studied in model bacterial species, including *Bacillus subtilis*, *Caulobacter crescentus*, and *Escherichia coli*. Here, we present an analysis of these complexes in an obligate intracellular bacterium with a highly reduced genome. *Orientia tsutsugamushi*, a cytoplasm-dwelling Gram-negative alphaproteobacterium, only retains a subset of proteins normally found in the elongasome and divisome. It also lacks all copies of the major peptidoglycan polymerase, Class A Penicillin Binding Protein, and has been shown to build an intermediate peptidoglycan cell wall-like structure that is low in abundance and insufficient to consistently confer a rod shape to the bacterium. We have carried out a first analysis of the elongasome and divisome in *Orientia tsutsugamushi*, quantifying the expression and subcellular localization of five key proteins through early stages of the intracellular infection cycle. We show how these are affected by antibiotic treatment and present a model for minimal elongation and division in an obligate intracellular bacterium.**

SIGNIFICANCE STATEMENT

- Bacterial cell elongation and division are driven by the elongasome and divisome, but these complexes are poorly understood in obligate intracellular species with reduced genomes.
- This study identifies and characterizes a minimal set of elongasome and divisome proteins in showing dynamic, stage-specific localization of FtsZ, FtsI, FtsQ, MreB, and PBP2 during intracellular growth, and their disruption by antibiotics targeting cell wall synthesis.
- These findings reveal how a minimal divisome-elongasome network can support bacterial replication within host cells, offering insight into the evolution of cell division under extreme genome reduction.

Monitoring Editor
Ethan Garner
Harvard University

Received: Dec 2, 2025
Revised: May 4, 2026
Accepted: May 20, 2026

INTRODUCTION

Bacterial cells are typically encased in an extensive cross-linked mesh of glycan strands and peptide side chains called peptidoglycan (Vollmer and Bertsche, 2008; Vollmer *et al.*, 2008). This confers shape to bacterial cells and protects them from high internal turgor pressure, as well as providing mechanical force to drive septation during cell division. Growing bacterial cells need to extend and divide this mesh without compromising structural integrity, which would lead to loss of protection and, therefore, cell lysis and death. These fundamental roles for the cell wall mean it is an effective target of multiple classes of antibiotics (Sarkar *et al.*, 2017). Elongation and septation of the peptidoglycan sacculus need to be coordinated with growth of the inner and, in the case of Gram-negative bacteria, outer membranes, as well as internal processes such as DNA replication and segregation. In most bacterial species, cell division is carried out by a multiprotein complex, the divisome, driven by the bacterial tubulin homolog FtsZ (Rowlett and Margolin, 2015; McQuillen and Xiao, 2020; Battaje *et al.*, 2023). In many nonspherical bacteria, an additional complex, the elongasome, drives elongation of the cell wall using the bacterial actin homolog MreB (Shi *et al.*, 2018).

Components of the bacterial divisome and elongasome are largely conserved across bacterial species, although there are differences in the exact timing and mechanism of recruitment as well as the presence of auxiliary and duplicate proteins (Caccamo and Brun, 2018). Assembly of the divisome can be broadly separated into three stages (McQuillen and Xiao, 2020). In most bacterial species, one of the first proteins to arrive at the site of future division is FtsZ, which polymerises in short filaments usually around the short axis in the middle of the cell (Rowlett and Margolin, 2015). Positioning of this Z-ring is regulated by different systems, for example, the MinCDE and nucleoid occlusion systems in *E. coli* and other species (Thanbichler, 2010; Cameron and Margolin, 2023), and MipZ in alphaproteobacteria (Thanbichler and Shapiro, 2006). FtsZ is anchored to the membrane via several FtsZ-binding proteins, the most ubiquitous of which is the actin homolog FtsA (Naha *et al.*, 2023). These early complexes recruit a second wave of components that primarily regulate Z-ring assembly and activation, and these include FtsB, FtsL, and FtsQ (Kashammer *et al.*, 2023; Nguyen *et al.*, 2023), as well as FtsK, a DNA translocase that pumps residual unsegregated DNA to the correct half of the cell before division (Aussel *et al.*, 2002; Stouf *et al.*, 2013). Finally, proteins involved in peptidoglycan synthesis arrive at the mid-cell position, including the activator FtsN, the Lipid II flippase MurJ, the glycosyltransferase FtsW, and the transpeptidase FtsI. Guided by the FtsZ filament, these peptidoglycan synthases drive peptidoglycan polymerisation around the septum of the cell, thus driving cell septation and fission (Barrows and Goley, 2021; Attaibi and den Blaauwen, 2022; Lamanna and Maurelli, 2022; Cameron and Margolin, 2023).

The bacterial elongasome is only present in nonspherical bacteria and is similarly assembled around a filament, in this case that of the actin homolog MreB (Shi *et al.*, 2018). MreB binds directly to membranes via an N-terminal amphipathic helix (Salje *et al.*, 2011), and interacts with the regulatory proteins RodZ, MreC, and MreD (Szwedziak and Lowe, 2013). This complex recruits the Lipid II flippase MurJ as well as a second set of glycosyltransferase and transpeptidase proteins, RodA and PBP2 (Zomorodipour and Andersson, 1999).

The divisome and elongasome complexes are broadly conserved across bacterial species and were likely present in the last bacterial common ancestor (Szwedziak and Lowe, 2013; Megrian *et al.*, 2022). However, there is diversity in the way these systems are deployed in diverse bacterial species (Caccamo and Brun, 2018). In obligate intracellular bacteria of the order Chlamydiales, which in some species, such as *C. trachomatis,* only assemble a peptidoglycan ring at the septum of dividing cells, FtsZ has been lost, and MreB is instead localized to the middle of the cell and coordinates cytokinesis (Frandi *et al.*, 2014; Jacquier *et al.*, 2014; Ouellette *et al.*, 2020). Within the alphaproteobacteria, there is diversity in the site of insertion of nascent peptidoglycan; for example, in the Rhizobiales, cell growth is driven at a single bacterial pole rather than better studied insertion along the length of the cell (Brown *et al.*, 2012). In members of the Neisseriaceae family, FtsZ drives cytokinesis, but septation occurs longitudinally along the long axis of the cell (Nyongesa *et al.*, 2022). Together, these examples demonstrate that the multi-protein complexes can be redeployed in different ways to achieve regulation of peptidoglycan synthesis, cell growth, and cell division.

Almost all of our knowledge about the elongasome and divisome comes from the study of free-living bacteria. Obligate intracellular bacteria have evolved to grow and divide exclusively within a living cell, and this has important implications for cell growth and division (Salje, 2021). Peptidoglycan is highly immunogenic, which risks leading to elimination of intracellular bacteria by activation of intracellular immune pathways, therefore bacteria that are committed to the intracellular replicative niche have evolved mechanisms to counter this threat (Otten *et al.*, 2018). Obligate intracellular bacteria are nutritional parasites that depend on host cells for metabolic precursors and intermediates, so it is expected that their growth and division would be coupled to the nutritional status of host cells. One extreme example of this is in the Mealybug endosymbiont *Moranella*, in which certain peptidoglycan synthesis genes have been transferred to the host chromosome, putting bacterial growth and division under direct control of host cells (Bublitz *et al.*, 2019). In addition to the example of *C. trachomatis* given above, cell division has been studied in the cytoplasmic obligate intracellular bacterium *Rickettsia parkeri*, in which the subcellular position of the FtsZ-binding protein ZapA was demonstrated (Figueroa-Cuilan *et al.*, 2023). Apart from these examples, very little is known about the timing and assembly of the elongasome and divisome in obligate intracellular bacteria, nor how this is affected by the cellular host. Our goal was to study this process using the cytoplasm-dwelling obligate intracellular bacterium *Orientia tsutsugamushi* (Ot).

This article was published online ahead of print in MBoC in Press (http://www.molbiolcell.org/cgi/doi/10.1091/mbc.E25-12-0574) on May 27, 2026.

#These authors contributed equally.

†Present address: Centre for Tropical Medicine and Global Health, Nuffield Department of Medicine, University of Oxford, OX3 7LG Oxford

Author contributions: Conceptualization: J.S.; Methodology: S.C., E.H., O.S.; Investigation: S.C., E.H., O.S.; Formal analysis: S.C., E.H., O.S.; Writing – original draft: J.S.; Writing – review & editing: all authors; Supervision: J.S.; Funding acquisition: J.S.

Conflict of interest: The authors declare no competing financial interest.

*Address correspondence to: Jeanne Salje (jss53@cam.ac.uk).

Abbreviations used: dcw, division and cell wall gene cluster; ICE, integrative and conjugative element; LPS, lipopolysaccharide; MIC, minimal inhibitory concentration; Ot, Orientia tsutsugamushi; PBP, penicillin binding protein; PG, peptidoglycan; RAGE, rickettsial amplified genetic element; SEDS, shape, elongation, division and sporulation

© 2026 Chuenklin *et al.* This article is distributed by The American Society for Cell Biology under license from the author(s). Twelve months after publication it is available to the public under an Attribution–Noncommercial–Share Alike 4.0 Unported Creative Commons License (http://creativecommons.org/licenses/by-nc-sa/4.0).

"ASCB®," "The American Society for Cell Biology®," and "Molecular Biology of the Cell®" are registered trademarks of The American Society for Cell Biology.

Ot is a Gram-negative obligate intracellular bacterium in the order Rickettsiales, family Rickettsiaceae (Salje, 2017; Luce-Fedrow *et al.*, 2018). It causes the vector-borne human disease scrub typhus and infects a range of cell types, including endothelial cells, dendritic cells, and macrophages (Luce-Fedrow *et al.*, 2018). Like all obligate intracellular bacteria, Ot has a highly reduced genome (Cho *et al.*, 2007; Nakayama *et al.*, 2008). However, its genome has been invaded by a highly proliferated integrative and conjugative element (ICE), the rickettsial amplified genetic element (RAGE), that comprises around 50% of the Ot genome (Lamanna and Maurelli, 2022; Lariviere and Goley, 2022; Kullapanich *et al.*, 2025). This has led to frequent chromosomal rearrangements, and the eight complete Ot genomes available to date completely lack synteny to one another (Batty *et al.*, 2018; Giengkam *et al.*, 2023). Given this highly dynamic genome, the presence of conserved microsynteny, where small groups of genes remain together in all genomes, reflects strong selective pressure, suggesting coordinated regulation and activity (Mika-Gospodorz *et al.*, 2020; Giengkam *et al.*, 2023).

Ot can be cultured in a range of cell types in vitro, with an infection cycle that lasts 4–7 d (Giengkam *et al.*, 2015; Salje, 2021). Bacteria are taken up by clathrin-mediated endocytosis and macropinocytosis (Atwal *et al.*, 2022), whereupon they escape membrane-bound compartments and reside free in the cytoplasm (Chu *et al.*, 2006). They traffic along microtubules to the perinuclear region (Kim *et al.*, 2001), where they undergo DNA replication beginning around 2 d post-infection (Giengkam *et al.*, 2015). Bacterial replication primarily occurs in a microcolony adjacent to the host nucleus. Beginning around 4 d post infection, individual bacteria traffic to the edge of the cell and bud off in a membrane-enclosed extracellular form ready for infection of a new host cell (Atwal *et al.*, 2022).

We previously showed that Ot builds a so-called intermediate peptidoglycan-like cell wall (Atwal *et al.*, 2017). This is low in abundance and difficult to detect, and levels fluctuate over the course of the intracellular infection cycle (Atwal *et al.*, 2022). Because of its low abundance, the bacteria are not always rod-shaped and can appear as spheres or other, ill-defined shapes. Ot lacks all Class A penicillin binding proteins (Atwal *et al.*, 2017; Otten *et al.*, 2018), bifunctional enzymes with peptidoglycan glycosyltransferase and transpeptidase activity (Popham and Young, 2003; Macheboeuf *et al.*, 2006; Sauvage *et al.*, 2008), and we previously showed that other host-associated bacteria had also specifically lost this class of enzymes whilst retaining other genes in the peptidoglycan biosynthesis pathway (Atwal *et al.*, 2021). Of those we tested, bacteria that had lost the Class A penicillin-binding proteins also built an intermediate cell wall that did not confer a rod-shaped form, and that was low in abundance (Atwal *et al.*, 2021). This may confer a selective advantage in the host-associated replicative niche through reduction of this immunogenic structure. The osmotically protective environment conferred by association with host cells likely enables the loss of a complete and structurally intact peptidoglycan cell wall.

In the current study, we sought to carry out the first characterization of the elongasome and divisome in an organism with a highly reduced and fragmented genome and a minimal peptidoglycan cell wall. Through this, we examine how extensive gene loss has led to the retention of only the core machinery required for elongation and division and how these processes are achieved in the context of replication within a eukaryotic cell.

RESULTS

Ot encodes a minimal set of genes involved in cell division and elongation

Given the irregular shape and unusual cell wall of Ot, we sought to determine which genes normally involved in cell division and the establishment of cell shape have been retained in this highly reduced genome. The overall structure of the cell envelope of Ot is shown in Figure 1A, with an outer membrane that lacks lipopolysaccharide (LPS) and a cell wall with only a minimal peptidoglycan-like sacculus. We searched in eight complete genomes of Ot (strains Boryong, Gilliam, Ikeda, Karp, Kato, UT76, UT176, TA686) for the presence or absence of divisome and elongasome genes using the well-studied and closely related free-living alpha proteobacterium *Caulobacter crescentus* complexes as a comparison (Figure 1, B and C; Table 1). Within the divisome, Ot has retained *dipI, sdpA, zapE, fzlA, ftsZ, ftsA, ftsK, ftsB, ftsL, ftsQ, ftsW, pbp3 (ftsI), murJ*, and *mraY*, but lacks *rodZ, fzlC, zauP, zapA, ftsN, ftsE, ftsX, dipM, sdpB,* and the Class A PBPs *pbpX and pbpY.* Whilst *amiC* is absent, predicted amidase activity is present through another amidase, *amiD,* not found in *C. crescentus*. Within the elongasome, Ot has retained *mreB, mreC, mreD, rodA, pbp2 (mrdA), murJ*, and *mraY* but lacks *rodZ.*

Cell division and cell wall biogenesis genes are located in small groups of genes dispersed across the Ot genome

The division and cell wall gene cluster (dcw) comprises a group of genes involved in cell division and cell wall biosynthesis that are encoded within one contiguous region in *E. coli*, and whose relative positions to one another are conserved in many bacterial species (Mingorance and Tamames, 2004; Pereira *et al.*, 2007; Kamran *et al.*, 2018). We found that the single contiguous dcw cluster of *E. coli* is separated into five groups in Ot (Figure 2A). Of these, *ftsA* and *ftsZ* have been moved into separate genetic loci, whereby *ftsZ* is now positioned adjacent to the lipid II biosynthesis gene *murA*. *ftsL, ftsI, murE, murF,* and *mraY* remain clustered in Ot as in *E. coli,* although the genes appear in a different order. *murD, ftsW,* and *murG* have been separated into one group, and *murC, murB, ddlB*, and *ftsQ* in another, consistent with relative positions in the hypothetical ancestral dcw cluster. We compared these groupings with those found in diverse bacterial species (Figure 2) and found that the dcw cluster is distributed into 1–9 loci in the species examined, with *ftsA* and *ftsZ* commonly found separated from the rest of the cluster.

We determined the relative positions of dcw genes, other genes involved in peptidoglycan biosynthesis, cell elongation, and cell division, and the abundant surface antigen *tsa56* across eight strains of Ot (Figure 2B). Whilst the relative positions of gene clusters varied as shown previously, there was strong conservation of the following groups of genes: *murA-ftsA, pbp2-mreB-rodA, ftsL-ftsI-murF-murE-mraY, mreB-mreC, murD-ftsW-murG, pbp2-mreB-rodA*, and *tsa56-murC-murB-ddl-ftsQ*. Given the high levels of gene movement in the Ot genome, these conserved microsynteny are likely to be significant in terms of coordinated expression and regulation.

Divisome proteins FtsZ, FtsI, and FtsQ, and elongasome proteins MreB and PBP2 have distinct patterns of subcellular localization in Ot

We sought to undertake an initial characterization of the divisome and elongasome machinery in Ot by determining the

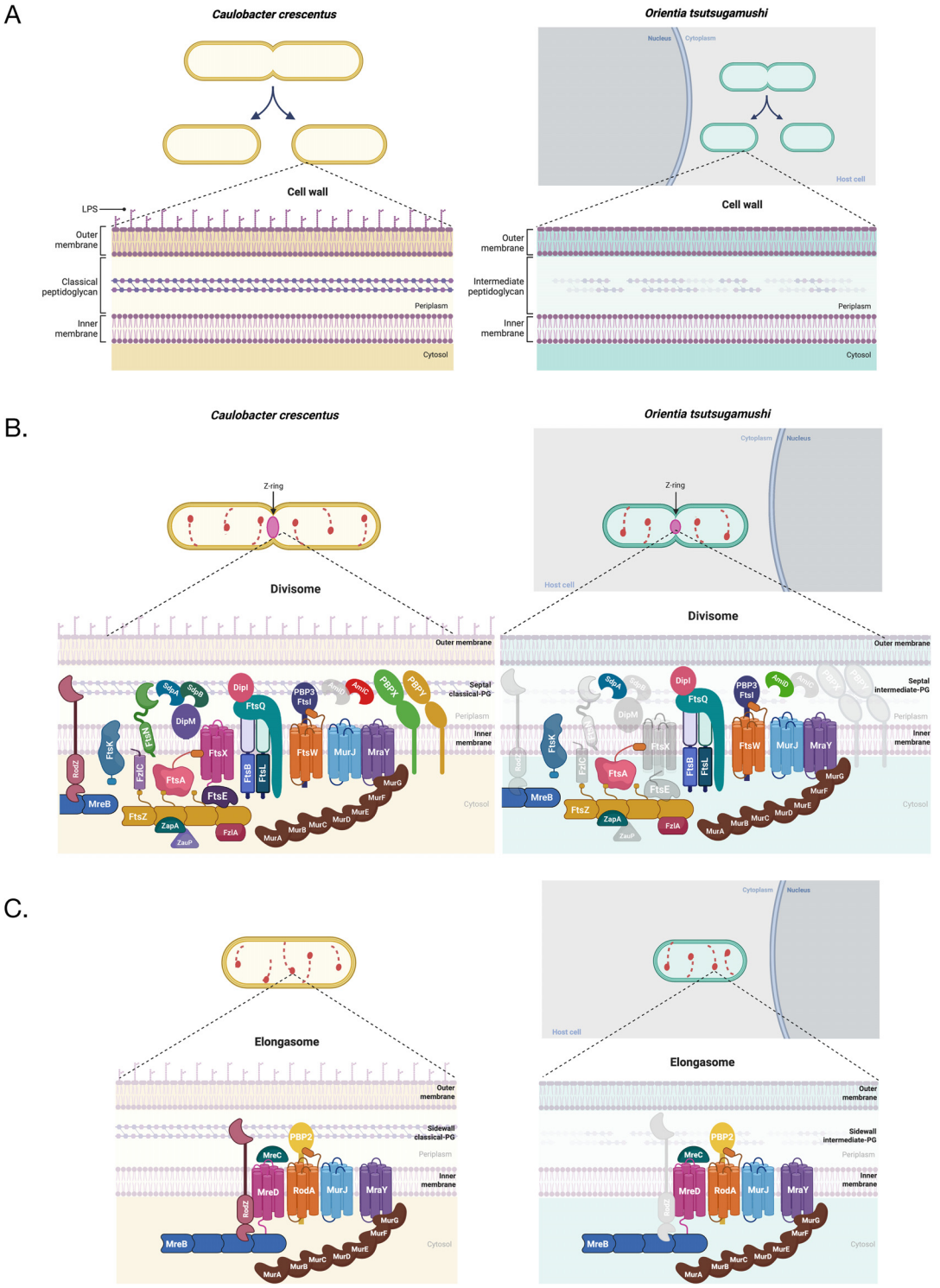


FIGURE 1: Schematic overview of the cell envelope and divisome/elongasome components present in Ot compared with *Caulobacter crescentus* A. Overview of the cell envelope of *C. crescentus* and Ot. Ot is a diderm bacterium that lacks LPS and produces only a minimal peptidoglycan-like cell wall. B. Major components of the bacterial divisome in *C. crescentus* and Ot. Note that AmiD is present in Ot but not *C. crescentus*, and whilst it is included here to demonstrate that amidase activity is conserved in Ot, it is not known whether it actually localizes to the mid-cell. C. Major components of the bacterial elongasome in *C. crescentus* and Ot. B was adapted from Lariviere and Goley (Lariviere and Goley, 2022), and all panels were produced on Biorender.com. Proteins present in each species are colored, and absent proteins are shown in gray.

Biological function(s)	Protein name[ii]	*E. coli*	*C. crescentus*	*O. tsutsugamushi*	Location
Lipid II precursor synthesis	MurA	✔	✔	✔	Cytoplasm
	MurB	✔	✔	✔	Cytoplasm
	MurC	✔	✔	✔	Cytoplasm
	MurD	✔	✔	✔	Cytoplasm
	MurE	✔	✔	✔	Cytoplasm
	MurF	✔	✔	✔	Cytoplasm
	MurG	✔	✔	✔	Cytoplasmic side of inner membrane
	Alr	✔	✔	X	Cytoplasm
	Ddl	✔	✔	✔	Cytoplasm
	MraY	✔	✔	✔	Inner membrane
Peptidoglycan synthases, putative flippases, and SEDS proteins	PBP1a (Class A PBP)	✔	✔	X	Elongasome/general PG synthesis
	PBP1b (Class A PBP)	✔	X	X	Divisome/repair PG synthesis
	PbpC (Class A PBP)	X	✔	X	Periplasm
	PbpX (Class A PBP)	X	✔	X	Periplasm
	PbpY (Class A PBP)	X	✔	X	Periplasm
	PbpZ (Class A PBP)	X	✔	X	Periplasm
	PBP2/MrdA (Class B PBP)	✔	✔	✔	Elongasome
	PBP3/FtsI/PbpA2 (Class B PBP)	✔	✔	✔	Divisome
	PBP5	✔	✔	X	Periplasm (cell wall maturation)
	FtsW (SEDS)	✔	✔	✔	Divisome
	RodA (SEDS)	✔	✔	✔	Elongasome
	MurJ	✔	✔	✔	Inner membrane
Peptidoglycan degradation, remodelling and recycling proteins	AmiA	✔	X	X	Divisome
	AmiB	✔	X	X	Divisome
	AmiC	✔	✔	X	Divisome
	AmiD	✔	X	✔	Periplasm (PG recycling)
	PBP4b	✔	X	✔	Periplasm
	DipM	X	✔	X	Periplasm/divisome associated
	SdpA	X	✔	✔	Periplasm
	SdpB	X	✔	X	Periplasm
Cell division/ morphogenesis proteins	FtsA	✔	✔	✔	Divisome
	FtsB	✔	✔	✔	Divisome
	FtsE	✔	✔	X	Divisome
	FtsH	✔	✔	✔	Inner membrane protease (global)
	FtsK	✔	✔	✔	Divisome
	FtsL	✔	✔	✔	Divisome
	FtsN	✔	✔	X	Divisome
	FtsP	✔	X	X	Divisome
	FtsQ	✔	✔	✔	Divisome
	FtsX	✔	✔	X	Divisome
	FtsY	✔	✔	✔	Inner membrane (SRP receptor)
	FtsZ	✔	✔	✔	Divisome
	MreB	✔	✔	✔	Elongasome
	MreC	✔	✔	✔	Elongasome
	MreD	✔	✔	✔	Elongasome
	RodZ	✔	✔	X	Elongasome
	EnvC	✔	X	X	Divisome
	ZipA	✔	X	X	Divisome
	ZapA	✔	✔	X	Divisome
	ZapB	✔	X	X	Divisome
	ZapE	✔	✔	✔	Divisome
Spatial regulators and accessory factors	LpoA	✔	X	X	Outer membrane lipoprotein
	LpoB	✔	X	X	Outer membrane lipoprotein
	NlpD	✔	X	X	Outer membrane lipoprotein
	EzrA	✔	X	X	Divisome regulator
	ParA	X	✔	✔	Cytoplasm
	ParB	X	✔	✔	Cytoplasm/chromosome
	PopZ	X	✔	X	Cell poles
	MipZ	X	✔	✔	Cytoplasm/divisome positioning

(*Continues*)

Biological function(s)	Protein name[ii]	*E. coli*	*C. crescentus*	*O. tsutsugamushi*	Location
Other	FzlA	X	✔	✔	Cytoplasm/divisome
	FzlC	X	✔	X	Inner membrane midcell/divisome
	ZauP	X	✔	X	Cytoplasm/divisome
	ZapT	X	✔	X	Cytoplasm/nucleoid
	DipI	X	✔	✔	Periplasm/inner membrane
	DalA	X	✔	X	Periplasm
	LdpF	X	✔	X	Periplasm/inner membrane
	TolQ	✔	✔	✔	Inner membrane
	TolR	✔	✔	✔	Inner membrane/periplasm
	TolA	✔	✔	✔	Inner membrane/periplasm
	TolB	✔	✔	✔	Periplasm
	Pal	✔	✔	✔	Outer membrane lipoprotein

TABLE 1: Summary of the presence and absence of proteins related to cell morphogenesis and PG biosynthesis and turnover in *Orientia tsutsugamushi* and *Escherichia coli*.

subcellular localization of key proteins within intracellular bacteria. We selected three divisome proteins (FtsZ, FtsI, and FtsQ) and two elongasome components (MreB and PBP2), and generated polyclonal antibodies against purified proteins or synthetic peptides.

Antibody specificity was first assessed by immunofluorescence microscopy following heterologous expression of the target proteins in *E. coli* (Supplemental Figure S1), and by immunoblotting of recombinant proteins (Supplemental Figure S2A) or native proteins (Supplemental Figure S2B). All antibodies produced a clear immunofluorescence signal in *E. coli* expressing the corresponding Ot protein (Supplemental Figure S1). However, PBP2 and MreB also yielded detectable signal in wild-type *E. coli* lacking exogenous Ot protein expression, potentially consistent with cross-reactivity against the endogenous homologues.

In immunoblot analyses of *E. coli* expressing recombinant Ot proteins, all antibodies except PBP2 detected a single band at the expected molecular weight (Supplemental Figure S2A). The PBP2 antibody produced only a weak band at the expected size despite a strong immunofluorescence signal, suggesting preferential recognition of a conformational epitope. Immunoblotting of native Ot lysates yielded clear bands of the expected size only for FtsZ and FtsQ (Supplemental Figure S2B), whereas the remaining antibodies detected lower molecular weight species, likely corresponding to degradation products. Given that Ot is not genetically tractable, direct validation by target depletion was not feasible; therefore, antibody validation primarily relied on heterologous expression in *E. coli*.

We used these antibodies to analyse the subcellular localization of FtsZ, FtsQ, FtsI, MreB, and PBP2 in the Ot strain Karp grown in monkey kidney epithelial Vero cells (growth curve shown in Supplemental Fig. S3). These cells were selected because bacteria grown in Vero cells gave the clearest antibody labeling of all cell lines tested. Using an antibody against the abundant surface protein TSA56 to delineate the outer membrane of bacteria, we determined the subcellular positions of these five proteins in individual bacterial cells (Figure 3A). Cells were scored as being rod-shaped, circular, or dividing (septum present). Proteins were classified as being dispersed in the cytoplasm ("cytoplasmic"), localized across the entire membrane ("membrane – complete"), localized in patches on the membrane ("membrane – partial"), or forming discrete foci at the poles ("foci – pole"), septum ("foci/ring – septal") or elsewhere ("foci – other"). In this way, bacteria fixed between 6 h and 3 d post-infection were classified with a shape and subcellular localization for each protein (Figure 3B). At 6 h the bacteria have entered host cells but are not yet replicative, whilst by 3 d post-infection, bacteria are metabolically active and dividing (Kullapanich *et al.*, 2025). It was not possible to analyse samples later than 3 d post-infection due to crowding caused by large numbers of intracellular bacteria.

FtsZ is a bacterial tubulin homolog that assembles into filaments at the site of cell division (Barrows and Goley, 2021). In *E. coli* and *C. crescentus*, it is one of the first proteins to arrive at the site of the future divisome (Bi and Lutkenhaus, 1991; Goley *et al.*, 2011). We found that FtsZ was present in all dividing cells and was primarily found at the septum or poles of dividing or rod-shaped cells. In circular cells, there is no observable pole, and the foci are located on the membrane.

FtsI is a Class B PBP that provides transpeptidase activity required for crosslinking Lipid II molecules within a peptidoglycan sacculus (Macheboeuf *et al.*, 2006; Sauvage *et al.*, 2008). It has a single transmembrane helix and a globular periplasmic domain that interacts with the SEDS (Shape, Elongation, Division, and Sporulation) glycosyltransferase protein FtsW (Kashammer *et al.*, 2023). It is homologous to PBP2 (MrdA; Macheboeuf *et al.*, 2006; Sauvage *et al.*, 2008). In *E. coli, C. crescentus*, and many other bacteria, FtsI is localized to the divisome, and PBP2 is primarily involved in elongasome activity (den Blaauwen *et al.*, 2017). We found that FtsI in Ot is localized either as a septal focus, primarily in dividing cells, or dispersed throughout the cytoplasm. Cytoplasmic localization of FtsI has not been previously described and is unexpected for a membrane protein.

FtsQ is a member of the FtsQLB trimeric complex (Nguyen *et al.*, 2023) that regulates the transpeptidase and transglycosylase activity of the FtsW-FtsI complex and thus controls the onset of divisome enzymatic activity (Tsang and Bernhardt, 2015). It is recruited by FtsK and is one of a middle group of proteins to arrive at the maturing divisome in *E. coli* (Du and Lutkenhaus, 2017). We found it to be primarily localized in the cytoplasm of Ot cells, with other cells exhibiting foci or patches on the membrane. Notably, we sometimes observed pairs of newly divided cells in which only one of the two daughter cells contained FtsQ, suggesting rapid proteolysis or protein segregation.

MreB is a bacterial actin homolog that forms short filaments perpendicular to the long axis of rod-shaped cells (van den Ent *et al.*, 2001; Domínguez-Escobar *et al.*, 2011; Garner *et al.*, 2011). These filaments rotate bidirectionally in a cell wall synthesis-dependent

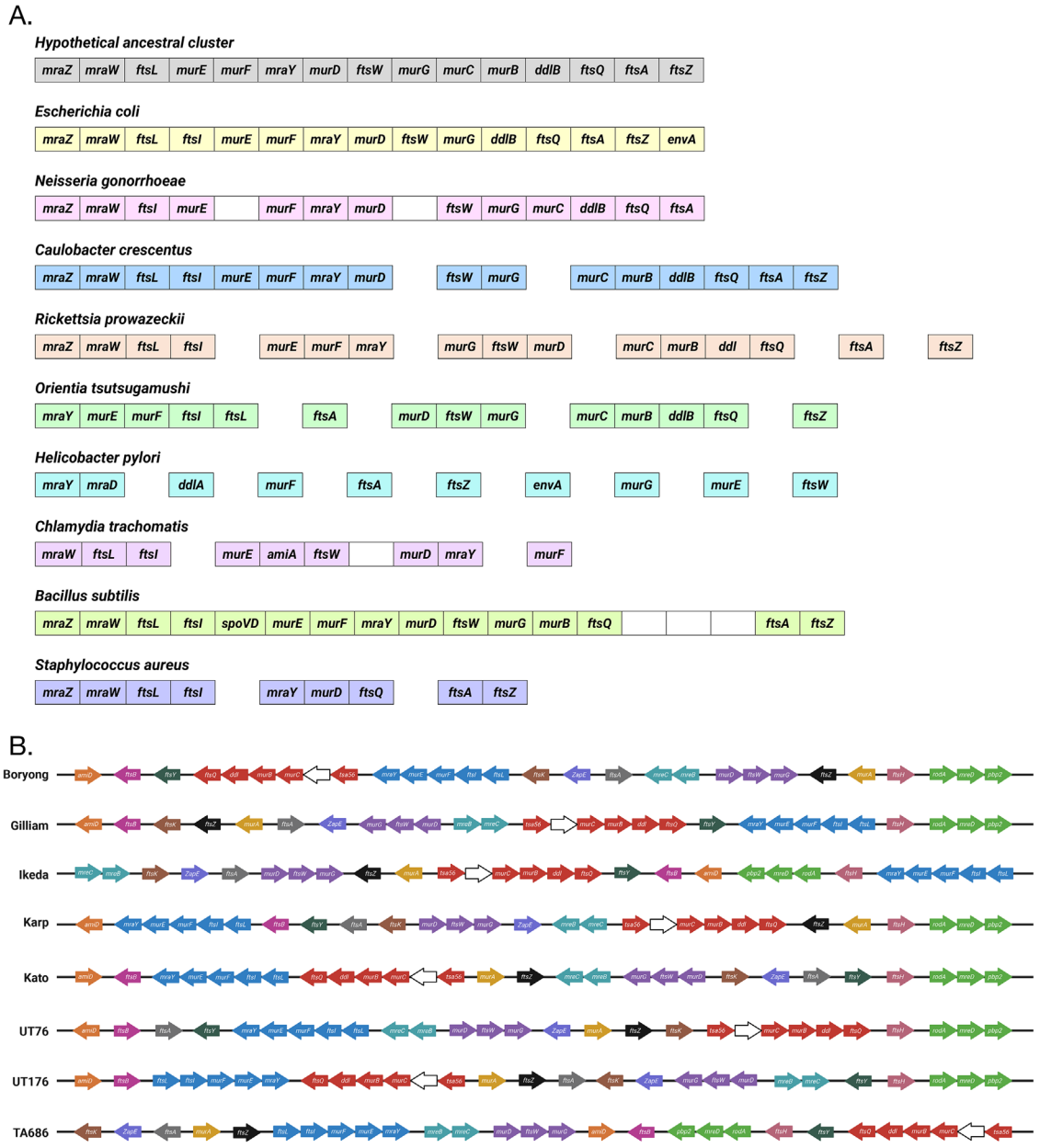


FIGURE 2: Genomic organization of cell division-related genes in Ot. A. Representative genes of the *dcw* cluster in various bacterial genomes. Connected boxes represent contiguous genes. White boxes represent genes absent in the hypothetical ancestral *dcw* cluster. Sets of genes split by spaces represent groups that are scattered in the genome. Only the major genes are displayed, and all isolated genes may not be shown. The genes in Ot are from strain Karp. B. Genomic organization of 25 genes involved in bacterial cell division and peptidoglycan cell wall synthesis and the major surface antigen *tsa56*, across eight diverse Ot strains. Adjacent arrow-shaped boxes in the same colour represent a group of neighbouring genes, while white ones are representatives of an unknown gene. Genomic distances between groups of genes or one or more genes of the same colour are not to scale.

manner (Domínguez-Escobar *et al.*, 2011; Garner *et al.*, 2011). MreB attaches to the inner surface of the cell membrane using an amphipathic helix (Salje *et al.*, 2011) and recruits and regulates the PBP2/RodA transpeptidase/transglycosylase complex via interactions with MreC and MreD (Cho *et al.*, 2016). MreB and/or PBP2 are generally positioned along the length of rod-shaped cells, but they also localise to the mid-cell or mid-cell adjacent region in some alphaproteobacterial under some conditions or stages of growth (Gitai *et al.*, 2004; Hocking *et al.*, 2012; Delaby *et al.*, 2025). In Ot, we observed that the majority of cells—of all morphologies—exhibited MreB localization dispersed throughout the cytoplasm. A small number of cells of all morphologies had MreB localized across the entire surface of the bacterium, presumably recruited to the inner surface of the inner membrane. As with FtsQ, we identified pairs of dividing cells in which MreB was only present in one of the two daughter cells.

PBP2 is a Class B PBP homologous to FtsI and usually involved in elongasome-peptidoglycan synthesis in rod-shaped cells

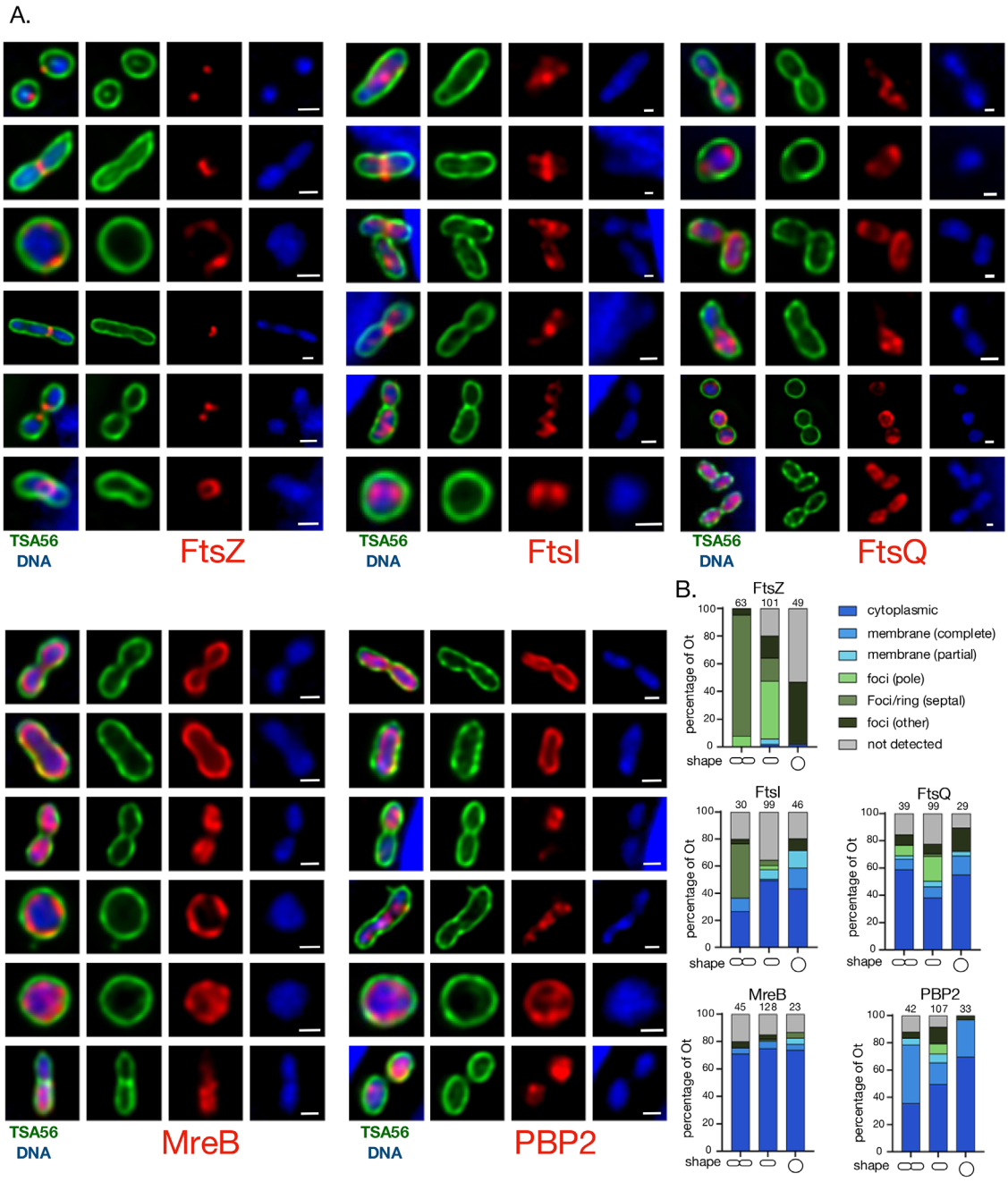


FIGURE 3: Subcellular localization of divisome and elongasome components in Ot. A. Immunofluorescence microscopy images of intracellular Ot labeled with antibodies against Ot FtsZ, FtsI, FtsQ, MreB, and PBP2. The bacterial outline is delineated by an antibody against the surface protein TSA56 (green). DNA is labeled with Hoechst (blue), and the divisome/elongasome protein of interest is in red. Images are taken between 6 h and 3 d post-infection and are selected to represent the range of subcellular protein distributions observed. Scale bar = 1 μm. B. Quantification of the distribution of different proteins classified according to bacterial shape. Bacteria were classified as rod-shaped, round, or dividing. In each bacterium, the subcellular position of the protein was manually classified as cytoplasmic, membrane (complete or partial), foci (pole, septal, or partial), or not detected. Quantification was performed on 30–128 (n) bacteria combined from 6, 24, 48, and 72 h post-infection, taken from one biological replicate, with the actual number used in each analysis shown above each bar in the graphs.

(Popham and Young, 2003; Macheboeuf *et al.*, 2006; Sauvage *et al.*, 2008). It is localized to small elongasome patches that move perpendicular to the long axis of a bacterium, driving cell wall synthesis and thus cell elongation (Garner *et al.*, 2011). Whilst we observed a small number of cells with the expected discrete foci on the membrane, the overwhelming majority of cells displayed PBP2 localization in either the cytoplasm or the entire inner membrane of the cell. The localization of PBP2 was highly similar to MreB, suggesting shared regulation and activity as described in other bacterial systems.

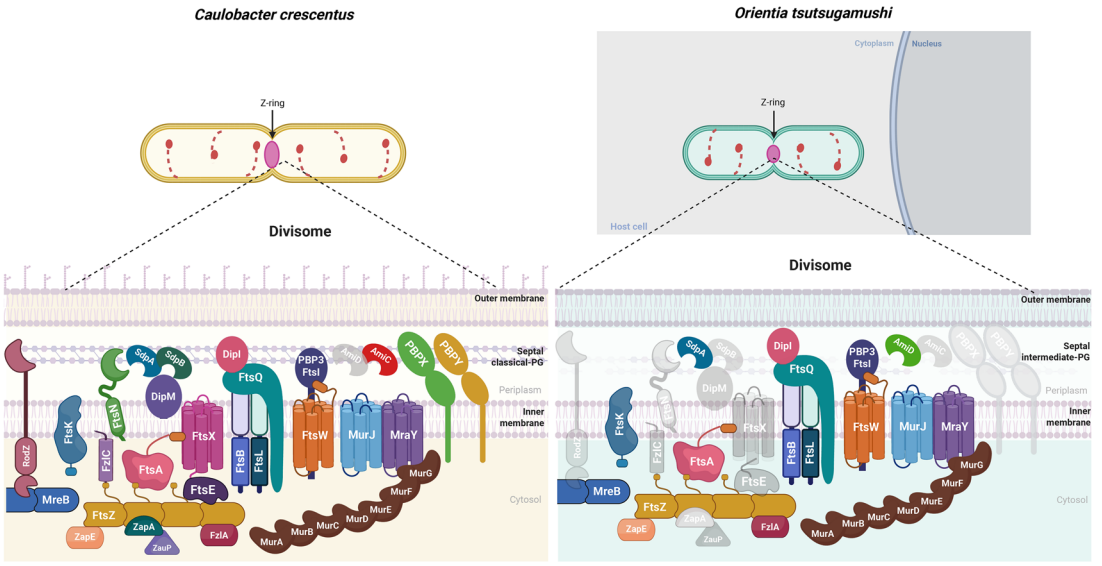


FIGURE 4: The subcellular localization of divisome and elongasome components changes over time. Quantification of the subcellular position of FtsZ, FtsI, FtsQ, MreB, and PBP2 in Ot at 6, 24, 48, and 72 h post-infection. Quantification was performed on 13–61 (n) bacteria from one biological replicate, with the actual number used in each analysis shown above each bar in the graphs.

The patterns of localization change over time

Having established overall localization patterns of FtZ, FtsI, FtsQ, MreB, and PBP2, we asked how the localization of these proteins changes over time. We quantified the distribution at 6-, 24-, 48-, and 72-h post-infection for each protein and observed that all changed over time. The most striking change was between 6- and 24-h post-infection. In all cases, the percentage of bacteria completely lacking a detectable signal was the highest at 6-h post-infection and decreased to almost 0% by 24 h post-infection, increasing again at 48- and 72-h post-infection. It was not possible to image intracellular bacteria after this time point due to the tightly packed microcolonies formed by Ot (North *et al.*, 2025). Both FtsQ and PBP2 exhibited the highest level of membrane localization at 24 h post-infection, a pattern that was most pronounced in PBP2.

An important caveat of this analysis is that, although infections were initially synchronized by the addition of bacteria, the starting inoculum likely contained cells at mixed stages of development, and synchrony is expected to decrease over time. In addition, technical constraints limited the size of the datasets obtained. Consequently, while these results indicate temporal changes in relative expression patterns, they should be interpreted qualitatively rather than quantitatively.

Antibiotic treatment induces changes in the localization of divisome and elongasome components

To further understand the observed patterns of subcellular localization, we asked how these patterns would change if the cell wall and elongasome complexes were disrupted. We first sought to disrupt the MreB filament using A22. We demonstrated that this compound was effective on intracellular Ot (Supplemental Figure S4A) and selected a working concentration of 25 µg/ml. At 3 d post-infection, treatment with A22 resulted in more circular Ot (Figure 5, A and B) and a decrease in the number of cells with detectable MreB (Figure 5C), consistent with the loss of elongasome activity. A small number of Ot cells were also observed to be abnormally long (Figure 5B), possibly suggesting additional disruption to divisome activity. These results were validated using a second MreB inhibitor, MP265, which produced a similar inhibition of bacterial growth as well as shape change in Ot at 25 µg/ml (Supplemental Figure S4C). The Ot cell wall was disrupted using phosphomycin, an inhibitor of MurA, an enzyme involved in the synthesis of the Lipid II precursor of peptidoglycan. Treatment with 300 µg/ml phosphomycin for 3 d caused Ot to become large and round (Figure 5, A and B), consistent with previous reports (Atwal *et al.*, 2017). This came with a dramatic change to the localization of the proteins investigated. The distinct localization patterns of FtsI, FtsQ, MreB, and PBP2 were lost, and all four proteins were instead primarily found in multiple punctae throughout the cytoplasm, a distribution unseen in untreated cells. FtsZ was the only protein to retain significant membrane localization, although the protein was often observed to form patches on the membrane rather than the smaller foci more commonly seen in the untreated condition. A significant proportion of bacteria also exhibited FtsZ localized in the punctate distribution observed with the other proteins. Whilst drug treatment experiments always carry the risk of effects being caused by off-target effects, stress responses, protein aggregation, or other indirect effects, the finding that A22, MP265, and phosphomycin all caused shape change strongly indicates that divisome/elongasome localisation is coupled to peptidoglycan synthesis.

DISCUSSION

Here, we demonstrate that the divisome proteins FtsZ, FtsI, and FtsQ, as well as the elongasome components MreB and PBP2, are expressed during the intracellular lifecycle of Ot. These proteins exhibit a range of distinct subcellular localizations that are sensitive to disruption of elongasome activity or inhibition of cell wall synthesis.

A limitation of our study is its reliance on antibody labeling, necessitated by the current lack of genetic tools for generating fluorescent fusion proteins in Ot. This raises the potential risk of off-target antibody binding. However, we consider this risk to be minimal for several reasons. First, we demonstrated that the

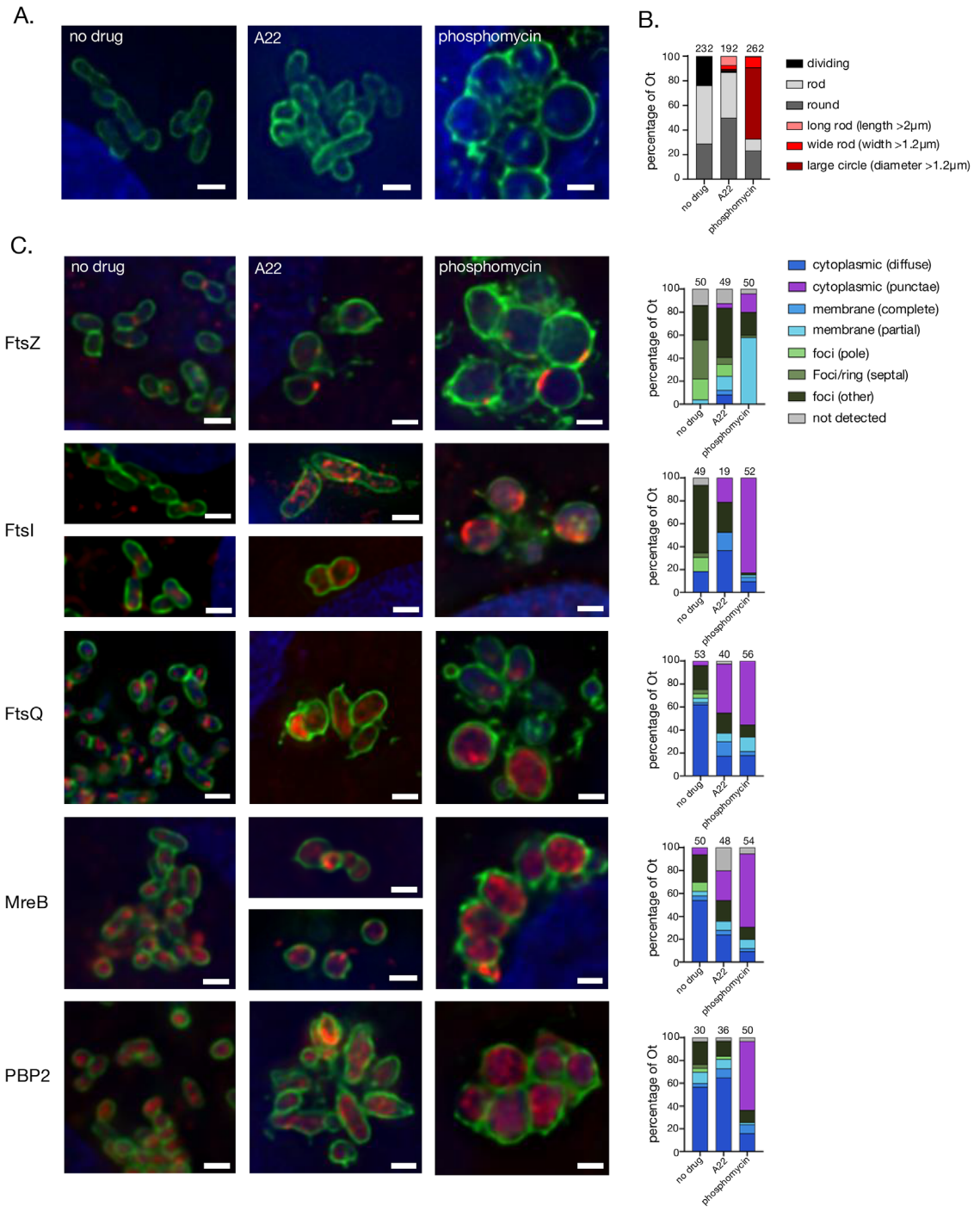


FIGURE 5: The subcellular localization of divisome and elongasome components is affected by perturbation of MreB filaments and the cell wall. A. Representative images of Ot in the presence of the MreB-targeting drug A22 (25 µg/ml) and the cell wall-targeting drug phosphomycin (300 µg/ml). Bacteria were labeled with an antibody against the surface protein TSA56 (green). Samples were stained with Hoechst to visualise host and bacterial DNA. Both drugs lead to a change in cell shape. Scale bar = 1 µm. B. Quantification of the subcellular position of FtsZ, FtsI, FtsQ, MreB, and PBP2 in Ot in the presence of A22 and phosphomycin at 72 h post-infection. Drugs were added at the concentrations above for 48 h before fixation. Quantification was performed on over 19–56 (n) bacteria, from one biological replicate, with the actual number used in each analysis shown above each bar in the graphs.

antibodies interact with the expected proteins through fluorescence microscopy of cognate proteins overexpressed in *E. coli* and by immunoblotting of recombinant proteins. Second, each antibody revealed a unique pattern of subcellular localization that varied across different stages of the infection cycle, arguing against nonspecific cytoplasmic recognition. Third, antibody signals were perturbed by pharmacological disruption of the elongasome and cell wall pathways, consistent with the intended targets. While we cannot completely exclude the possibility of off-target effects, the cumulative evidence supports the specificity of our reagents. Nonetheless, future validation using genetically encoded fusions will be important.

A second limitation of this study lies in the labor-intensive and low-throughput nature of imaging individual bacteria within host cells. Because imaging and analysis had to be performed manually, the number of cells that could be feasibly examined was restricted. As a result, we were unable to systematically include biological replicates, although comparable observations were made independently by different researchers. For this reason, the data are presented as illustrating general trends in protein localization rather than providing precise quantitative measurements. Given the sensitivity of obligate intracellular bacteria to variables such as host cell confluence, media composition, and growth conditions, some variation in the exact distribution and timing of localization is expected. Nevertheless, robust features—such as the septal localization of FtsZ—are unlikely to be affected by these differences.

FtsZ and FtsI localize to the mid-cell in dividing Ot, consistent with roles in septation. By contrast, the localization pattern of FtsQ is more diffuse and rarely shows a clear septal focus. As a member of the conserved FtsQLB complex—typically recruited by early division proteins such as FtsZ and responsible for activating late divisome components like FtsI—this atypical localization may indicate that in Ot, FtsQ is not restricted to the division site but is instead activated specifically when at the septum.

MreB and PBP2 exhibited two main localization patterns: diffuse cytoplasmic or membrane-associated. These patterns differ from the short, membrane-bound filaments typically observed for MreB in other bacteria (Domínguez-Escobar *et al.*, 2011; Garner *et al.*, 2011). In most systems, MreB forms dynamic filaments along the inner membrane, which are tightly associated with active peptidoglycan synthesis. The absence of such structures in Ot raises important questions about the nature, orientation, and regulation of MreB filaments and their interaction with PBP2. Notably, Ot MreB possesses an extended N-terminal domain with a weaker predicted amphipathic helix compared with that from other bacteria (Supplemental Figure S5), potentially reducing its membrane affinity and contributing to the predominantly cytoplasmic localization. This suggests that additional regulatory mechanisms or conformational changes may be required to mediate membrane association and filament formation.

The localization of elongasome components MreB and PBP2 along the bacterial perimeter, together with the restriction of divisome components FtsZ and FtsI to the septum of rod-shaped cells, leads us to propose a model for shape change and division in Ot. Here, we show that a subset of Ot cells is large and spherical. We propose that membrane-associated MreB drives the transition from these large, round cells to a rod-shaped morphology. This transition may be mediated by the collective effect of multiple MreB filaments inducing membrane curvature and/or by peptidoglycan synthesis directed by PBP2. The peripheral localization of PBP2, along with the observation that inhibition of peptidoglycan synthesis with phosphomycin results in enlarged, round cells, supports a role for peptidoglycan in this process. Once a rod shape is established, FtsZ, FtsI, and other divisome components can assemble at the septum to initiate cell division. Consistent with this model, septal localization of FtsZ and FtsI is observed only in rod-shaped, dividing cells and not in round cells. This model would restrict peptidoglycan synthesis to those bacteria actively undergoing cell division, potentially contributing to immune evasion in an obligate intracellular bacterium. The model is summarized in Figure 6 and will be explored further in future studies.

Unexpectedly, we observed that both FtsQ and PBP2 localized within the cytoplasm in some cells, despite being single-pass membrane proteins. Several possible scenarios exist that might explain this: (1) the observed proteins may be incompletely translated and still associated with ribosomes, (2) cytoplasmic chaperones such as SecB may transiently retain them before membrane insertion, though this has not been reported for integral membrane proteins, or (3) the proteins may be undergoing degradation, although this is unlikely given that membrane protein degradation typically occurs at the membrane. The observation that multiple membrane-associated proteins—including MreB—are often found in the cytoplasm suggests that Ot may regulate their activity through cytoplasmic sequestration. This would represent a form of temporal regulation adapted to Ot's intracellular lifecycle, in which cell wall synthesis is restricted to specific stages. Supporting this, we sometimes observed asymmetric localization of FtsQ, MreB, and PBP2 in dividing cells, with these proteins present in only one half of the bacterium, often in a cytoplasmic state. Such striking binary localization supports a model in which cytoplasmic sequestration and possibly proteolysis act as additional regulatory layers for cell wall synthesis proteins. A fourth explanation is possible, namely that the unexpected localization results from nonspecific binding of antibodies. Future studies will be required to confirm the localization patterns and test these hypotheses directly.

While the localization of FtsZ and FtsI is broadly consistent with established models from other bacterial systems, the patterns observed for MreB, PBP2, and FtsQ are distinctly different. These differences align with Ot's atypical cell biology. Ot possesses a minimal and poorly detectable cell wall (Atwal *et al.*, 2017), insufficient for consistently generating a rod shape and likely evolved to reduce exposure to host immune responses. Recent work has shown that Ot undergoes a biphasic developmental cycle, transitioning to an extracellular form with reduced levels of peptidoglycan-like fragments and a predominantly round, rather than rod shape (Atwal *et al.*, 2022). This supports the idea that cell wall synthesis is tightly regulated throughout the infection cycle. Our findings suggest that this regulation may be achieved, at least in part, through the spatial control of protein localization.

In summary, this study provides the first characterization of divisome and elongasome components in Ot, revealing dynamic and unconventional patterns of subcellular localization. This work lays the foundation for future studies to further dissect these regulatory pathways.

MATERIALS AND METHODS

Cells and bacteria

Vero C1008 African green monkey kidney epithelial cells (CRL1586) were used for this study. Cells were grown at 37°C and 5% CO_2 in Life Technologies DMEM, high glucose (41965039, Life Technologies), supplemented with 10% heat-inactivated fetal bovine serum (HI FBS; 16140071, Life Technologies). Ot strain Karp was used for

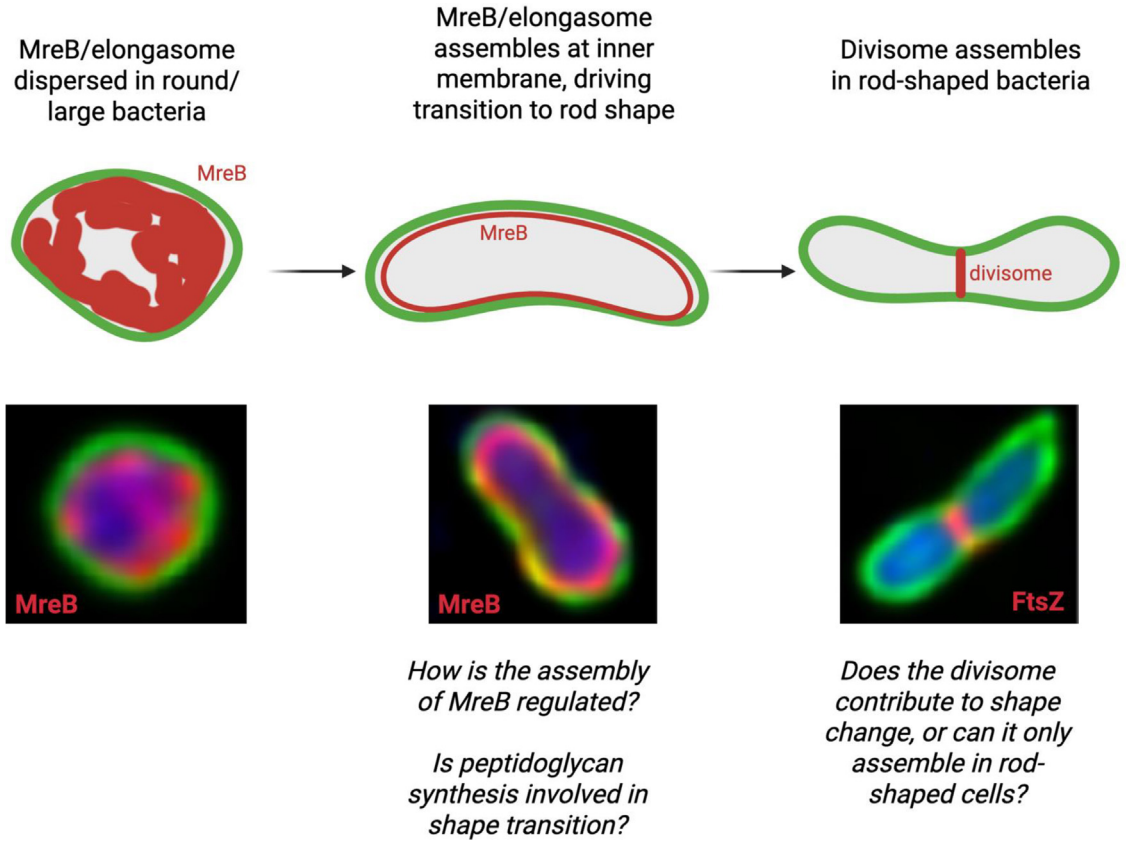


FIGURE 6: Proposed model for shape determination in Ot. The schematic shows a possible model for the transition from round/pleiomorphic bacteria to rod-shaped bacteria in Ot. In this model, MreB is either absent or cytoplasmic in non-rod-shaped bacteria. Assembly of MreB at the cytoplasmic membrane would lead to a transition to rod shape using force from MreB assembly and potentially also peptidoglycan synthesis. The divisome would then assemble at the septum of rod-shaped bacteria and drive bacterial division. Open questions relating to the model are shown in the figure.

infections. Frozen stocks of bacteria were prepared as described previously (Giengkam *et al.*, 2015).

DNA extraction and qPCR

To extract bacterial DNA, host cells were lysed with alkaline lysis buffer and heated at 95°C for 30 min as previously described (Giengkam *et al.*, 2015). qPCR analysis was carried out using a Bio-Rad CFX96 Real-Time System C1000 Touch Thermal Cycler (1855196, Bio-Rad) and the primers and probes outlined in Supplemental Table S1, as previously described (Giengkam *et al.*, 2015; Salje, 2025).

Bacterial growth tests

A growth curve was used to determine the viability and infectivity of the prepared frozen stock (Supplemental Figure S3). Vero cells in a 24-well culture plate (142475, Thermo Fisher Scientific) were infected with 4.76×10^5 Ot. The media was changed 6 h post-infection to remove residual extracellular bacteria. At the time of sample collection, the DNA in each well was collected as described above, and the number of bacteria per well was calculated using qPCR against the single copy *16s* gene. The minimum inhibitory concentration (MIC) of the drugs used in this study, phosphomycin and A22, was determined by assessing bacterial replication with a dose-response curve (Supplemental Figure S4). Bacteria were added to each well of a 48-well plate (150687, Thermo Fisher Scientific) containing Vero cells. At 24 h post-infection, the media was changed, and phosphomycin (P5396, Sigma-Aldrich), A22 (SML0471, Sigma-Aldrich), or MP265 (Cambridge Bioscience, T24494) were added at the indicated concentrations. Ot copy number per well was calculated after 5 d of infection using qPCR to quantify the Ot *tsa47* gene. Supplemental Figures S3 and S4 were produced using GraphPad Prism 9 for macOS Version 9.3.1. Biological replicates were plotted as individual points, and bar height was set as the mean of the replicates, with the error bar representing ± one SD.

Production of slides for immunofluorescence microscopy

µ-Slide 8 Well ^{high} Glass Bottom chamber slides (80807, ibidi GmbH, Germany) were coated with 100 ug/ml Poly-D-Lysine solution (A003E, Merck Millipore) by shaking for at least 6 h before seeding with Vero cells. The cells were infected with an MOI of 4.96 (timecourse experiment) or 11.58 (drug treatment experiment), as measured by number of bacteria quantified by qPCR. 24 h post-infection, media was removed and either replaced with fresh media only (timecourse experiment and no-drug control), or media containing MP265 (25 µg/ml), A22 (25 µg/ml), or phosphomycin (300 µg/ml). Slides were fixed at the appropriate point in the time course, or 48 h post-antibiotic treatment. Media was removed, the slides were washed with PBS, and fixed with 4% formaldehyde solution (28906, Thermo Scientific) for 10 min at room temperature.

Antibody name	Sequence of immunogen[i]	Immunogen type	Host and antibody type	NCBI Accession# and amino acid position	Concentration (mg/mL)
TSA56 (in-house)	KLTPPQPTIMPISIADRDF -KLH	Synthetic peptide from strain Karp coupling with KLH carrier protein	Rat, monoclonal	WP_045912668.1, K132-F150	Unknown
FtsI[ii]	KDYKNFVGHYNVQEIFMYSSN IGIVQIGLDIGQFNLKKYFKLLA LDKILKIELPEKANSLYHANTSW NNITTATISYGYGISISPLHFVQA MIPIVNGGNLYPITLIKRTPNDN LIAQKIFSSKTSKELNSLLRLAVK HGTSKNSDVVGYLVGGKVGTA KKIKDRKYDKNSIRSSFIGIYPSIA PKFIIYLMLD	Recombinant protein from strain Gilliam	Rabbit, polyclonal	WP_052692488.1, K330-D523	2.80
FtsQ	RLEKVIIDGQQNVTTDKVIAAIN ADTGTPIFDIDIYAVKERLEQNS WIRNVVIERRLPNTIYVGILERKP IAIWQLNKRLYLIDNEGIVLHTD KVSAFSSLLHLVGQGANLHAN QLILTISSEPNLASKIVSAVRYGN RRWNLIFQENIVVKMPESDFNK AWQYLVKLFQSDKFFNQKYKV LDLRDSSKYYIEYYN	Recombinant protein from strain Gilliam	Rabbit, polyclonal	SPR11039.1, R80-N276	2.90
FtsZ	KNSGIINNKPQKDD-C -KLH KATEDNDSQVASDG-C -KLH	Synthetic polypeptide from strain Gilliam coupling with KLH carrier protein	Rabbit, polyclonal	WP_109234839.1 K373-D386, K426-G439	1.24
MreB	FKSAEEMIKHFIHSVHNRRSFAG PVIIICVPSGSTPVERRAIQEAAE SAGGREVFLIEEPMAAAIGAGL PVTSPTGSMIVEIGGGTTQVAV LSLGGVVYSKSVRVGGDKMDE AISSYIRRYHNLLIGDPTAERIKK EIAT	Recombinant protein from strain Gilliam	Rabbit, polyclonal	WP_047220642.1, F90-T230	2.45
PBP2	ARGLKVRELDTIPSIPGKDIALSI DVNLQNKLYEMFDDRVGAAIL TDVNTGKIKALVSVPGYNINAFP RRISTKDWKALLDNPNLPLVSRA SQSLYPPGSIFQLVTVLAALEAG VNSKLTVYCNGKSFMNDTNFS CWNHRGHGNVDMLSAIKYSC NSYIYHLASLIGYNAILAMARKL GFWRRAVVNLPNELVGNLPTPE WKKRKTKQRWMLGDTLNIAIG QGYITTTPLQLARMITSIANGKQ LLQLSLTLDEDGYHKNLNINAG HIDFIRQALKAIINNESSGTAYSL HSDKTKLMISGKTCSAQVGSSL QAHGLFIG	Recombinant protein from strain Gilliam	Rabbit, polyclonal	WP_047220114.1, A221-G540	3.42

TABLE 2: Primary antibodies used in this study. All of the antibodies (except TSA56) were produced by ABclonal Technology (USA) and purified by Antigen Affinity Chromatography.

Slides were again washed with PBS and stored at 4°C until further processing.

Immunofluorescence microscopy

Slides were permeabilized on ice using absolute ethanol (445730010, Thermo Fisher Scientific, France) for 30 min followed by 0.5% Triton-X-100 (85112, Thermo Fisher Scientific, USA) for 30 min. The antibodies in Table 2 were diluted 1:200 in 1 mg/ml Bovine Serum Albumin (BSA; A9647, Sigma-Aldrich) in PBS and added to relevant wells of the permeabilized cells for 3 h at 37°C. Following this, slides were washed with PBS and incubated with the secondary antibodies detailed in Table 3 for 1 h at 37°C. Slides were washed with PBS and stored in mounting media (20 mM Tris-HCl, pH 8.0, 0.5% N- N-propyl-gallate, and 90% glycerol) at 4°C until imaging.

Samples were imaged using a Nikon Eclipse Ti2-E microscope and NIS-Elements AR Version 5.42.03. For samples with few bacteria (Figure 3A), individual bacteria were imaged to create Z-stacks,

Antibody/dye	Target	Working dilution in PBS	Manufacturer	Product code
Goat anti-Rabbit IgG (H+L) Highly Cross-Adsorbed Secondary Antibody, Alexa Fluor™ Plus 555	Antibodies bound to POI (in Table 2)	1:500	Thermo Fisher Scientific	A32732
Goat anti-Rat IgG (H+L) Cross-Adsorbed Secondary Antibody, Alexa Fluor™ 488	Anti-TSA56 antibody (see Table 2)	1:500	Thermo Fisher Scientific	A11006
Hoechst 33342	Host and bacterial DNA	1:1000 (of 10 mg/ml solution)	Thermo Fisher Scientific	H1399

TABLE 3: Secondary antibodies and dyes used in this study.

before using maximum-intensity projection (maxIP) to generate a 2D image, which was deconvolved. For samples with more bacteria (Figure 5, A and C), clumps of bacteria were captured in Z-stacks, which were deconvolved using 3D deconvolution. MaxIP was then used to generate an image representative of protein distribution throughout the bacteria.

Image analysis

Bacterial morphology was determined by the appearance of the outer membrane protein TSA56. Under drug treatment conditions, the morphology of some cells deviated significantly from that of the untreated Ot. These were classified as long rods (length greater than 2 µm), wide rods (width greater than 1 µm), or large circles (diameter greater than 1.2 µm). The presence or absence of the protein of interest was recorded for individual bacterial cells. In those expressing the protein, its intracellular localization was identified by comparing its position relative to the TSA56 outline. Localization was manually sorted into the following categories: cytoplasmic, membrane (complete), membrane (partial), foci (pole), ring/foci (septal), foci (other), and cytoplasmic punctae. "Cytoplasmic" was used when the protein was spread uniformly throughout the cytoplasm, while "cytoplasmic punctae" denotes cells in which the cytoplasm was filled with foci of the protein of interest. At least 50 bacteria were counted for all conditions, except those where there were too few bacteria to reach this threshold, for example, at early timepoints before bacterial replication or following antibiotic treatment. Bacterial counts and proportions were calculated using Microsoft Excel Version 2508 and RStudio Version 2025.05.1-513, and plotted with GraphPad Prism 10.6.1. Statistical testing was carried out as detailed in the figure caption using GraphPad Prism 10.6.1.

Bioinformatic analysis

Past work from Otten *et al.* (2018) was extended by comparing the components of the divisome and elongasome proteins in Ot with *C. crescentus* (Table 1). The *dcw* gene cluster of Ot (strain Karp) was also analyzed using Geneious Prime software version 2023.2.1. This was compared with other bacteria as previously described (Battaje *et al.*, 2023) to generate Figure 2A. In light of recent work from Giengkam *et al.* (2023), the cell division proteins FtsB and FtsL were updated to be present in Ot, which were previously reported as absent by Otten *et al.* (2018).

The orientation and position of genes in the *dcw* cluster were then compared between 8 strains of Ot to generate Figure 2B. These strains were: Boryong (NCBI accession number NC009488.1), Gilliam (LS398551.1), Ikeda (NC_010793.1), Karp (LS398548.1), Kato (LS398550.1), UT76 (LS398552.1), UT176 (LS398547.1), and TA686 (LS398549.1; 5).

SDS–PAGE and immunoblotting

Solutions containing each of the proteins of interest (Supplemental Figure S3A) were obtained using a cell-free expression system (NEBExpress Cell-free *E. coli* Protein Synthesis System, E5306) following the manufacturer's instructions using plasmids expressing recombinant Ot proteins with a terminal 6xHis tag and lacking transmembrane helices, where applicable (except for OtPBP2fl). Ot lysates (Supplemental Figure S3B) were obtained by isolating bacteria from infected host cells as described above, before lysing the final bacterial pellet in a solution of RIPA buffer (Thermo Fisher Scientific, 89900) with added protease inhibitor (Thermo Fisher Scientific, 78439). The resultant solutions were boiled at 95°C for 5 min and loaded onto Mini-PROTEAN TGX Precast Protein Gels, 4%–15% (Bio-Rad, 4561086 or 4561083) for electrophoresis. Proteins were then transferred onto a nitrocellulose membrane (Cytiva, 10600011) and probed with the antibodies detailed in Table 2 and Supplemental Table S2. Primary antibodies were incubated overnight at 4°C, and secondary antibodies were incubated at room temperature for 30 min. Antibodies were diluted in PBS with 2% BSA. Before each antibody incubation, membranes were washed with rocking three times for 5 min in PBS–Tween 0.1% (Sigma-Aldrich, P2287). After the final incubation, membranes were similarly washed using PBS. Membranes were imaged using the BioRad Chemidoc, and the molecular weight of individual bands was calculated using the relative location of bands in the protein standard (NEB, P7719S).

Antibody testing in *E. coli*

Plasmids expressing recombinant Ot proteins, lacking transmembrane helices where applicable, were transformed into the BL21 strain of *E. coli* by heat shock and selected for by antibiotic exposure to 50 µg/ml Kanamycin Sulphate (Sigma-Aldrich, 60615).

Transformed *E. coli* were grown to an optical density at 600 nm (OD_{600}) 0.4–0.6 at 37°C in Luria Bertani (LB) media with 50 µg/ml Kanamycin Sulphate. Recombinant protein expression was induced with 400µM isopropyl β-D-1-thiogalactopyranoside (IPTG; FluoroChem, M02726) for 2 h under the same growth conditions. Bacteria were then adhered to a Poly L-Lysine (Sigma-Aldrich, P8920) coated slide and fixed with 1% vol/vol formaldehyde in phosphate-buffered saline (PBS) for 20 min at room temperature. Slides were washed three times in PBS, then permeabilized with 0.1% wt/vol Triton X-100 for 45 min at room temperature, washed thrice again, and then further permeabilized with 1 mg/ml lysozyme (SigmaAldrich, L6876) and 5 mM EDTA (EDTA) for another 45 min at room temperature. After three more washes, samples were blocked with 4% BSA for 30 min at room temperature, followed by incubation with 1:1000 primary antibody

targeting the relevant recombinant protein for 1 h at 37°C. Following this, samples were washed three times, and then incubated for 1 h at 37°C in a mixture of 1:1000 Alexa488-conjugated goat anti-rabbit secondary antibody (Thermo Fisher Scientific, A-11008) along with 1:1000 Hoechst (as described above) and 1:1000 of 5 mg/ml stock FM 4-64FX (Invitrogen, F34653), which was used as an *E. coli* membrane counterstain. After three more washes, samples were covered in mounting media and imaged as described above.

REFERENCES

Attaibi M, den Blaauwen T (2022). An updated model of the divisome: regulation of the septal peptidoglycan synthesis machinery by the divisome. Int J Mol Sci 23: 3537.

Atwal S, Chuenklin S, Bonder EM, Flores J, Gillespie JJ, Driscoll TP, Salje J (2021). Discovery of a diverse set of bacteria that build their cell walls without the canonical peptidoglycan polymerase aPBP. MBio 12: e0134221.

Atwal S, Giengkam S, Chaemchuen S, Dorling J, Kosaisawe N, VanNieuwenhze M, Sampattavanich S, Schumann P, Salje J (2017). Evidence for a peptidoglycan-like structure in *Orientia tsutsugamushi*. Mol Microbiol 105: 440–452.

Atwal S, Wongsantichon J, Giengkam S, Saharat K, Pittayasathornthun YJ, Chuenklin S, Wang LC, Chung T, Huh H, Lee SH, *et al*. (2022). The obligate intracellular bacterium *Orientia tsutsugamushi* differentiates into a developmentally distinct extracellular state. Nat Commun 13: 3603.

Aussel L, Barre FX, Aroyo M, Stasiak A, Stasiak AZ, Sherratt D (2002). FtsK Is a DNA motor protein that activates chromosome dimer resolution by switching the catalytic state of the XerC and XerD recombinases. Cell 108: 195–205.

Barrows JM, Goley ED (2021). FtsZ dynamics in bacterial division: what, how, and why? Curr Opin Cell Biol 68: 163–172.

Battaje RR, Piyush R, Pratap V, Panda D (2023). Models versus pathogens: how conserved is the FtsZ in bacteria? Biosci Rep 43: BSR20221664.

Batty EM, Chaemchuen S, Blacksell S, Richards AL, Paris D, Bowden R, Chan C, Lachumanan R, Day N, Donnelly P, *et al*. (2018). Long-read whole genome sequencing and comparative analysis of six strains of the human pathogen *Orientia tsutsugamushi*. PLoS Negl Trop Dis 12: e0006566.

Bi EF, Lutkenhaus J (1991). FtsZ ring structure associated with division in *Escherichia coli*. Nature 354: 161–164.

den Blaauwen T, Hamoen LW, Levin PA (2017). The divisome at 25: the road ahead. Curr Opin Microbiol 36: 85–94.

Brown PJ, de Pedro MA, Kysela DT, Van der Henst C, Kim J, De Bolle X, Fuqua C, Brun YV (2012). Polar growth in the Alphaproteobacterial order Rhizobiales. Proc Natl Acad Sci USA 109, 1697–1701.

Bublitz DC, Chadwick GL, Magyar JS, Sandoz KM, Brooks DM, Mesnage S, Ladinsky MS, Garber AI, Bjorkman PJ, Orphan VJ, *et al*. (2019). Peptidoglycan production by an insect-bacterial mosaic. Cell 179: 703-712.e7

Caccamo PD, Brun YV (2018). The molecular basis of noncanonical bacterial morphology. Trends Microbiol 26: 191–208.

Cameron TA, Margolin W (2023). Insights into the assembly and regulation of the bacterial divisome. Nat Rev Microbiol 22: 33-45

Cho H, Wivagg CN, Kapoor M, Barry Z, Rohs PDA, Suh H, Marto JA, Garner EC, Bernhardt TG (2016). Bacterial cell wall biogenesis is mediated by SEDS and PBP polymerase families functioning semi-autonomously. Nat Microbiol 1: 16172.

Cho NH, Kim HR, Lee JH, Kim SY, Kim J, Cha S, Kim SY, Darby AC, Fuxelius HH, Yin J, *et al*. (2007). The *Orientia tsutsugamushi* genome reveals massive proliferation of conjugative type IV secretion system and host-cell interaction genes. Proc Natl Acad Sci USA 104: 7981–7986.

Chu H, Lee JH, Han SH, Kim SY, Cho NH, Kim IS, Choi MS (2006). Exploitation of the endocytic pathway by *Orientia tsutsugamushi* in nonprofessional phagocytes. Infect Immun 74: 4246–4253.

Delaby M, Yang L, Jacq M, Gallagher KA, Kysela DT, Hughes V, Pulido F, Veyrier FJ, VanNieuwenhze MS, Brun YV (2025). Phenotypic plasticity in cell elongation among closely related bacterial species. Nat Commun 16: 5099.

Domínguez-Escobar J, Chastanet A, Crevenna AH, Fromion V, Wedlich-Söldner R, Carballido-López R (2011). Processive movement of MreB-associated cell wall biosynthetic complexes in bacteria. Science 333: 225–228.

Du S, Lutkenhaus J (2017). Assembly and activation of the *Escherichia coli* divisome. Mol Microbiol 105: 177–187.

van den Ent F, Amos LA, Löwe J (2001). Prokaryotic origin of the actin cytoskeleton. Nature 413: 39–44.

Figueroa-Cuilan WM, Irazoki O, Feeley M, Smith E, Nguyen T, Cava F, Goley ED (2023). Quantitative analysis of morphogenesis and growth dynamics in an obligate intracellular bacterium. Mol Biol Cell 34: ar69.

Frandi A, Jacquier N, Théraulaz L, Greub G, Viollier PH (2014). FtsZ-independent septal recruitment and function of cell wall remodelling enzymes in chlamydial pathogens. Nat Commun 5: 4200.

Garner EC, Bernard R, Wang W, Zhuang X, Rudner DZ, Mitchison T (2011). Coupled, circumferential motions of the cell wall synthesis machinery and MreB filaments in *B. subtilis*. Science 333: 222–225.

Giengkam S, Blakes A, Utsahajit P, Chaemchuen S, Atwal S, Blacksell SD, Paris DH, Day NP, Salje J (2015). Improved quantification, propagation, purification and storage of the obligate intracellular human pathogen *Orientia tsutsugamushi*. PLoS Negl Trop Dis 9: e0004009.

Giengkam S, Kullapanich C, Wongsantichon J, Adcox HE, Gillespie JJ, Salje J (2023). *Orientia tsutsugamushi*: comprehensive analysis of the mobilome of a highly fragmented and repetitive genome reveals the capacity for ongoing lateral gene transfer in an obligate intracellular bacterium. mSphere 8: e0026823.

Gitai Z, Dye N, Shapiro L (2004). An actin-like gene can determine cell polarity in bacteria. Proc Natl Acad Sci USA 101: 8643–8648.

Goley ED, Yeh YC, Hong SH, Fero MJ, Abeliuk E, McAdams HH, Shapiro L (2011). Assembly of the *Caulobacter* cell division machine. Mol Microbiol 80: 1680–1698.

Hocking J, Priyadarshini R, Takacs CN, Costa T, Dye NA, Shapiro L, Vollmer W, Jacobs-Wagner C (2012). Osmolality-dependent relocation of penicillin-binding protein PBP2 to the Division Site in *Caulobacter crescentus*. J Bacteriol 194: 3116–3127.

Jacquier N, Frandi A, Pillonel T, Viollier PH, Greub G (2014). Cell wall precursors are required to organize the chlamydial division septum. Nat Commun 5: 3578.

Kamran M, Dubey P, Verma V, Dasgupta S, Dhar SK (2018). Helicobacter pylori shows asymmetric and polar cell divisome assembly associated with DNA replisome. FEBS J 285: 2531–2547.

Kashammer L, van den Ent F, Jeffery M, Jean NL, Hale VL, Lowe J (2023). Cryo-EM structure of the bacterial divisome core complex and antibiotic target FtsWIQBL. Nat Microbiol 8: 1149–1159.

Kim SW, Ihn KS, Han SH, Seong SY, Kim IS, Choi MS (2001). Microtubule- and dynein-mediated movement of Orientia tsutsugamushi to the microtubule organizing center. Infect Immun 69: 494–500.

Kullapanich C, Aylward F, Jackson R, Salje J (2025). Developmental progression and single-cell heterogeneity of *Orientia tsutsugamushi* during intracellular infection. 2025.12.09.693123.

Lamanna MM, Maurelli AT (2022). What is motion? Recent advances in the study of molecular movement patterns of the peptidoglycan synthesis machines. J Bacteriol 204: e0059821.

Lariviere PJ, Goley ED (2022). Cell division in *Caulobacter crescentus*: a molecular-scale model. In: Cell Cycle Regulation and Development in Alphaproteobacteria, ed. E Biondi, Cham, Switzerland: Springer International Publishing, 101–141.

Luce-Fedrow A, Lehman M, Kelly D, Mullins K, Maina A, Stewart R, Ge H, John H, Jiang J, Richards A (2018). A review of scrub typhus (*Orientia tsutsugamushi* and related organisms): then, now, and tomorrow. Tropical Medicine and Infectious Disease 3: 8.

Macheboeuf P, Contreras-Martel C, Job V, Dideberg O, Dessen A (2006). Penicillin binding proteins: key players in bacterial cell cycle and drug resistance processes. FEMS Microbiol Rev 30: 673–691.

McQuillen R, Xiao J (2020). Insights into the structure, function, and dynamics of the bacterial cytokinetic FtsZ-ring. Annu Rev Biophys 49: 309–341.

Megrian D, Taib N, Jaffe AL, Banfield JF, Gribaldo S (2022). Ancient origin and constrained evolution of the division and cell wall gene cluster in Bacteria. Nat Microbiol 7: 2114–2127.

Mika-Gospodorz B, Giengkam S, Westermann AJ, Wongsantichon J, Kion-Crosby W, Chuenklin S, Wang LC, Sunyakumthorn P, Sobota RM, Subbian S, *et al*. (2020). Dual RNA-seq of Orientia tsutsugamushi informs on host-pathogen interactions for this neglected intracellular human pathogen. Nat Commun 11: 3363.

Mingorance J, Tamames J (2004). The bacterial dcw gene cluster: an island in the genome? In: Molecules in Time and Space: Bacterial Shape, Division and Phylogeny, ed. M Vicente, J Tamames, A Valencia, and J Mingorance, Boston, MA: Springer US, 249–271.

Naha A, Haeusser DP, Margolin W (2023). Anchors: A way for FtsZ filaments to stay membrane bound. Mol Microbiol 120: 525–538.

Nakayama K, Yamashita A, Kurokawa K, Morimoto T, Ogawa M, Fukuhara M, Urakami H, Ohnishi M, Uchiyama I, Ogura Y, *et al.* (2008). The Whole-genome sequencing of the obligate intracellular bacterium Orientia tsutsugamushi revealed massive gene amplification during reductive genome evolution. DNA Res 15: 185–199.

Nguyen HTV, Chen X, Parada C, Luo AC, Shih O, Jeng US, Huang CY, Shih YL, Ma C (2023). Structure of the heterotrimeric membrane protein complex FtsB-FtsL-FtsQ of the bacterial divisome. Nat Commun 14: 1903.

North AJ, Sharma VP, Pyrgaki C, S.y. JL, Atwal S, Saharat K, Wright GD, Salje J (2025). A comparison of super-resolution microscopy techniques for imaging tightly packed microcolonies of an obligate intracellular bacterium. J Microsc 301: 187–205.

Nyongesa S, Weber PM, Bernet E, Pulido F, Nieves C, Nieckarz M, Delaby M, Viehboeck T, Krause N, Rivera-Millot A, *et al.* (2022). Evolution of longitudinal division in multicellular bacteria of the *Neisseriaceae* family. Nat Commun 13: 4853.

Otten C, Brilli M, Vollmer W, Viollier PH, Salje J (2018). Peptidoglycan in obligate intracellular bacteria. Mol Microbiol 107: 142–163.

Ouellette SP, Lee J, Cox JV (2020). Division without binary fission: cell division in the FtsZ-less Chlamydia. J Bacteriol 202: e00252-20.

Pereira SFF, Henriques AO, Pinho MG, de Lencastre H, Tomasz A (2007). Role of PBP1 in cell division of *Staphylococcus aureus*. J Bacteriol 189: 3525–3531.

Popham DL, Young KD (2003). Role of penicillin-binding proteins in bacterial cell morphogenesis. Curr Opin Microbiol 6: 594–599.

Rowlett VW, Margolin W (2015). The bacterial divisome: ready for its close-up. Philos Trans R Soc Lond B Biol Sci 370: 20150028.

Salje J (2017). Orientia tsutsugamushi: a neglected but fascinating obligate intracellular bacterial pathogen. PLoS Pathog 13: e1006657.

Salje J (2021). Cells within cells: Rickettsiales and the obligate intracellular bacterial lifestyle. Nat Rev Microbiol 19: 375–390

Salje J (2025). Quantifying *Orientia tsutsugamushi* and other Rickettsiales bacteria by real time qPCR.

Salje J, van den Ent F, de Boer P, Lowe J (2011). Direct membrane binding by bacterial actin MreB. Mol Cell 43: 478–487.

Sarkar P, Yarlagadda V, Ghosh C, Haldar J (2017). A review on cell wall synthesis inhibitors with an emphasis on glycopeptide antibiotics. Medchemcomm 8: 516–533.

Sauvage E, Kerff F, Terrak M, Ayala JA, Charlier P (2008). The penicillin-binding proteins: structure and role in peptidoglycan biosynthesis. FEMS Microbiol Rev 32: 234–258.

Shi H, Bratton BP, Gitai Z, Huang KC (2018). How to build a bacterial cell: MreB as the Foreman of *E. coli* construction. Cell 172: 1294–1305.

Stouf M, Meile JC, Cornet F (2013). FtsK actively segregates sister chromosomes in *Escherichia coli*. Proc Natl Acad Sci USA 110: 11157–11162.

Szwedziak P, Lowe J (2013). Do the divisome and elongasome share a common evolutionary past? Curr Opin Microbiol 16: 745–751.

Thanbichler M (2010). Synchronization of chromosome dynamics and cell division in bacteria. Cold Spring Harb Perspect Biol 2: a000331.

Thanbichler M, Shapiro L (2006). MipZ, a spatial regulator coordinating chromosome segregation with cell division in *Caulobacter*. Cell 126: 147–162.

Tsang M-J, Bernhardt TG (2015). A role for the FtsQLB complex in cytokinetic ring activation revealed by an ftsL allele that accelerates division. Mol Microbiol 95: 925–944.

Vollmer W, Bertsche U (2008). Murein (peptidoglycan) structure, architecture and biosynthesis in *Escherichia coli*. Biochim Biophys Acta 1778: 1714–1734.

Vollmer W, Blanot D, de Pedro MA (2008). Peptidoglycan structure and architecture. FEMS Microbiol Rev 32: 149–167.

Zomorodipour A, Andersson SG (1999). Obligate intracellular parasites: *Rickettsia prowazekii* and *Chlamydia trachomatis*. FEBS Lett 452: 11–15.